Journal of Alloys and Compounds 619 (2015) 719–725

Contents lists available at ScienceDirect

Journal of Alloys and Compounds

journal homepage: www.elsevier.com/locate/jalcom

Ferromagnetism in single-valent manganites

I.O. Troyanchuk [a,*], M.V. Bushinsky [a], V. Sikolenko [b,c], V. Efimov [c], N.V. Volkov [d], D.M. Többens [b], C. Ritter [e], B. Raveau [f]

[a] Scientific-Practical Materials Research Centre NAS of Belarus, P. Brovki str. 19, 220072 Minsk, Belarus
[b] Helmholtz-Zentrum Berlin, Hahn-Meitner-Platz 1, 14109 Berlin, Germany
[c] Joint Institute for Nuclear Research, Joliot-Curie 6, 141980 Dubna, Russia
[d] Kirensky Institute of Physics, Akademgorodok 50, bld. 38, 660036 Krasnoyarsk, Russia
[e] Institut Laue-Langevin, 6 rue Jules Horowitz, BP 156, 38042 Grenoble Cedex 9, France
[f] Laboratoire CRISMAT, UMR 6508 associée au CNRS, ISMRA et Universite de Caen 6, Boulevard du Marechal Juin, 14050 Caen Cedex, France

ARTICLE INFO

Article history:
Received 13 August 2014
Accepted 27 August 2014
Available online 18 September 2014

Keywords:
Magnetically ordered materials
Solid state reactions
Exchange and superexchange
Magnetic measurements
Neutron diffraction

ABSTRACT

Structural and magnetization measurements have been performed on the $La_{0.7}Sr_{0.3}Mn_{0.85}Nb^{5+}_{0.15-x}Mg^{2+}_{x}O_3$ stoichiometric compounds. With rise of the Mg^{2+} content the formal oxidation state manganese increases from +3 ($x = 0$) up to +3.55 ($x = 0.15$). The compositions with $0 \leqslant x \leq 0.08$ undergo a structural transition from rhombohedral to orthorhombic symmetry below room temperature whereas $x = 0.1$ and $x = 0.15$ compounds are rhombohedral down to 2 K. The structural parameters evidence that the orthorhombic phase is not long-range orbitally ordered and that the structural transition is associated with a steric effect. The Mg-free compound is ferromagnetic with the Curie point of around 150 K and a magnetic moment of 3.1 μ_B/Mn. The substitution of Nb^{5+} with Mg^{2+} leads to a gradual weakening of the ferromagnetic component while in the $x = 0.15$ compound A-type antiferromagnetic short-range order is stabilized in spite of macroscopic $R\bar{3}c$ symmetry. All the compositions show insulating behavior. It is suggested that ferromagnetism is originated from superexchange interactions via oxygen. Covalence enhances the positive part of the superexchange interactions whereas structural disorder induced by Nb^{5+} and Mg^{2+} ions leads to suppression of ferromagnetism.

© 2014 Elsevier B.V. All rights reserved.

1. Introduction

$La_{1-x}A_xMnO_3$ (A = Ca, Sr, Ba) manganites have been of interest for many years since they exhibit very intriguing magnetic and magnetotransport properties [1–3]. In order to explain the interplay between magnetic and transport properties Zener introduced a special form of exchange interactions through charge carriers – double exchange [2]. De Gennes [4] developed a theory of double exchange and predicted that a canted magnetic structure forms at intermediate concentrations between the antiferromagnetic and ferromagnetic states. However, nuclear magnetic resonance data strongly support the mixed phase scenario as two different hyperfine lines corresponding to ferromagnetic and antiferromagnetic regions were observed [5–7]. Neutron diffraction and small angle neutron scattering data seem to be as well better understood assuming a mixed two phase state too [8–12]. The two phase picture is in agreement with a magnetization study [13] and recent theoretical considerations [14]. Besides it was found that the ferromagnetic state can be realized even in compounds containing only manganese of valence 3 [9,12,15–22]. For example the parent $LaMnO_3$ exhibits ferromagnetic interactions in the orbitally disordered phase ($T > 750$ K) with an approximated Curie point around 160 K [18]. Long-range ferromagnetism is observed in the $LaMn_{1-x}Ga_xO_3$ ($0.2 < x < 0.6$) and $LaMn_{1-x}Cr_xO_3$ ($0.2 < x < 0.6$) series containing only Mn^{3+} species [12,15–20]. Both these series show a gradual transition into an orbitally disordered state upon Ga^{3+} ($x > 0.5$) or Cr^{3+} ($x > 0.35$) substitution.

In the superexchange model, the ferromagnetic fraction of the exchange is determined by a virtual electron transfer from half-filled e_g-orbitals of Mn^{3+} ions to empty ones [20]. The static Jahn–Teller effect leads to an anisotropy of the superexchange interactions in parent $LaMnO_3$ [17,18,20]. Goodenough has proposed arguments for the ferromagnetism in orbitally disordered state to be caused by orbital fluctuations [17,18,20]. This has been suggested to be due to superexchange interactions between dynamically disordered Jahn–Teller Mn^{3+} centers, where the electronic configuration (e_g orbital occupancy) at the Mn^{3+} sites follows the vibrational motion, with the axis of the ferromagnetic interactions rotating rapidly with respect to the spin relaxation

* Corresponding author.
E-mail address: troyan@physics.by (I.O. Troyanchuk).

http://dx.doi.org/10.1016/j.jallcom.2014.08.236
0925-8388/© 2014 Elsevier B.V. All rights reserved.

time as the direction of the Jahn–Teller distortion is dynamically exchanged between the local x, y and z axes. In this picture a ferromagnetic component can arise from a local orbital disordering under doping. However, NPD studies did not reveal a coexistence of orbitally disordered and orbitally ordered phases in $LaMn_{1-x}Ga_xO_3$ ($0.2 < x < 0.5$) in spite of the presence of a ferromagnetic component [12]. In [15] it was shown that the ferromagnetic component found in the Ga-doped compounds is destroyed under pressure. This was ascribed to the breakdown of the magnetic ordering due to a structural transition from an orthorhombic into a rhombohedral phase. According to [15] $LaMnO_3$ and $LaMn_{0.5}Ga_{0.5}O_3$ become rhombohedral (space group $R\bar{3}c$) above 11 GPa and 8 GPa respectively. Rhombohedral symmetry does not allow a cooperative static Jahn–Teller distortion. So it has been suggested that ferromagnetism can occur in the d_{z^2}-orbitally ordered state by mixing of e_g-orbitals with different symmetry while orbital disorder leads to the frustration of magnetic interactions [15].

This is in apparent contradiction to the fact that ferromagnetism is very strong in the orbitally-disordered phases of $LaMn_{1-x}Ga_xO_3$ ($x = 0.6$) and $LaMn_{1-x}Cr_xO_3$ ($0.35 < x < 0.6$) [12,19]. External pressure stabilizes antiferromagnetism in the orthorhombic (*Pnma*) phase as it was evidenced by *ac*-magnetic susceptibility measurements for $LaMnO_3$ [15] and by neutron powder diffraction (NPD) for optimally doped manganites [23]. Increasing the external pressure up to 11 GPa the Neel point of $LaMnO_3$ rises from 140 K to 190 K [15]. In disagreement with [15] $LaMnO_3$ does not according to [24,25] undergo a structural transition into the rhombohedral phase but remains orthorhombic up to 35–40 GPa. $LaMnO_3$ and $LaMn_{0.8}Ga_{0.2}O_3$ exhibit transition from orthorhombic *Pnma* into orthorhombic *Imma* symmetry above 11 GPa [25,26]. High pressure, low temperature Raman measurements performed on $LaMnO_3$ up to 34 GPa provided the experimental evidence for the persistence of the local Jahn–Teller distortion over the entire stability range of the insulating phase [27]. In [15] it was shown that the ferromagnetic component in $LaMn_{0.5}Ga_{0.5}O_3$ strongly decreases within orthorhombic (*Pnma*) crystal structure which is stable up to 8 GPa. So the suppression of the ferromagnetic component under pressure seems to result from an enhancement of the antiferromagnetic part of interactions within the orthorhombically distorted structure. Note that the pressure induced decrease in the amplitude of the *ac*-magnetic susceptibility of $LaMnO_3$ [15] can be related to the structural transition into a more symmetric phase which does not allow weak ferromagnetism inherent to antiferromagnetic $LaMnO_3$ at ambient pressure. The antiferromagnetic interactions arising from the $3t_{2g}$ electrons of Mn^{3+} ion cannot be frustrated in the perovskite lattice in any space group. High pressure can enhance these interactions in larger extent than ferromagnetic interactions from the single e_g electron. Moreover it was reported [21] that under high pressure prepared formally Mn^{4+} free rhombohedral manganites exhibit ferromagnetism with the Curie point well above room temperature. All these different experimental results indicate that the understanding of the development of ferromagnetic interactions in manganites is still far from being clear. Moreover recent theoretical consideration [28] has provided arguments that the ferromagnetism of doped manganites is not caused by the double exchange interaction because the calculated T_C values are too small compared with the observed ones.

Optimally doped $La_{0.7}Sr_{0.3}(Mn^{3+}_{0.7}Mn^{4+}_{0.3})O_3$ has the highest critical temperature ($T_C = 380$ K) of the transition into the ferromagnetic state among mixed-valence manganites. The substitution of manganese with a two-valence ion such as Mg^{2+} leads to an increasing Mn^{4+}/Mn^{3+} ratio and enhances the role of the interactions between Mn^{3+}–Mn^{4+} pairs. Conversely, by replacing manganese ions with five-valence ions such as Nb^{5+} or Sb^{5+} the average manganese valence is lowered and, hence, Mn^{3+}–O–Mn^{3+} superexchange interactions via oxygen should be dominant. In this work we report the structure and properties of $La_{0.7}Sr_{0.3}Mn_{0.85}Nb_{0.15-x}Mg_xO_3$ series. In this series the formal oxidation state of manganese ions is changed from +3 ($x = 0$) up to +3.55 ($x = 0.15$) assuming oxygen stoichiometry. Our results indicate that superexchange interactions can be dominant in the formation of ferromagnetic state of studied manganites.

2. Experimental

Ceramic samples of $La_{0.7}Sr_{0.3}Mn_{0.85}Nb_{0.15-x}Mg_xO_3$ series were prepared by a solid-state reaction technique using high purity oxides La_2O_3, Mn_2O_3, Nb_2O_5, MgO and carbonate $SrCO_3$ taken in a stoichiometric ratio and thoroughly mixed in a planetary mill (Retsch, 300 rpm, 30 min). La_2O_3 was preliminary annealed at 1100 °C in air in order to remove moisture. The synthesis was performed at 1500–1550 °C for 7 h in air, using a two-step procedure with an interim annealing at 1400 °C for 5 h followed by a thorough grinding. The samples were cooled from the synthesis temperature with a rate of 300 °C/h down to 300 °C. The reference compound $La_{0.7}Sr_{0.3}Mn_{0.85}Ga_{0.15}O_3$ (gallium is in the three-valent state) have been prepared in a similar manner. Neutron powder diffraction (NPD) measurements of the $x = 0$ and $x = 0.15$ compounds were performed on the high intensity D1B ($\lambda = 2.520$ Å) and high resolution D2B ($\lambda = 1.594$ Å) diffractometers (Institute Laue-Langevin, Grenoble). The samples $x = 0.05$; 0.08 and 0.1 were studied with Fine Resolution Powder Diffractometer E9 (FIREPOD) ($\lambda = 1.7982$ Å) at the Helmholtz–Zentrum for Materials and Energy, Berlin. Rietveld refinement of data has been performed using FULLPROF soft package [29]. Magnetic properties of samples were investigated with PPMS set-up in magnetic fields up to 14 T and in the temperature range 5–320 K (Cryogenic Ltd.).

3. Results

Magnetization dependencies on magnetic field at 5 K are shown in Fig. 1. The evolution of a ferromagnetic component upon increasing Mg-doping is clearly evident. The compositions $x = 0$ and 0.05 have approximately equal magnetization at $T = 5$ K. For the compositions $x = 0.1$ and $x = 0.15$ spontaneous magnetization is significantly smaller than that for $x = 0$. The coercive field for $x = 0$ and $x = 0.05$ is around 0.01 T at 5 K and weakly increases with magnesium content increasing. Magnetic moments per manganese ion evaluated from magnetization data are around 3.5 μ_B ($x = 0$) and 0.6 μ_B ($x = 0.15$, first cycle of measurements). The observed magnetic moment for Mg-free compound is close to the expected value for the purely ferromagnetic state. One can suggest that the compositions $0 < x < 0.1$ are predominantly ferromagnetic. However, the presence of nonferromagnetic clusters embedded in a ferromagnetic matrix cannot be excluded. The contribution from nonferromagnetic clusters increases as the content of magnesium and therefore of Mn^{4+} ions rises. The Nb-free compound ($x = 0.15$) exhibits a gradual metamagnetic transition in the external magnetic field as can be seen from the field dependence of the magnetization in Fig. 2. The fact that the hysteresis loop is not symmetric indicates that this transition is partially irreversible. The second magnetic field cycle leads then to a smaller magnetic hysteresis. The magnetic moment in a field of 14 T is significantly

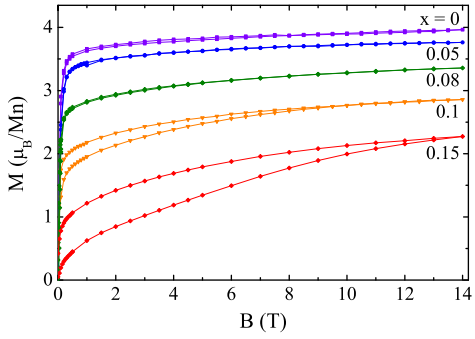

Fig. 1. Field dependencies of magnetization for $La_{0.7}Sr_{0.3}Mn_{0.85}Nb_{0.15-x}Mg_xO_3$ samples measured at 5 K.

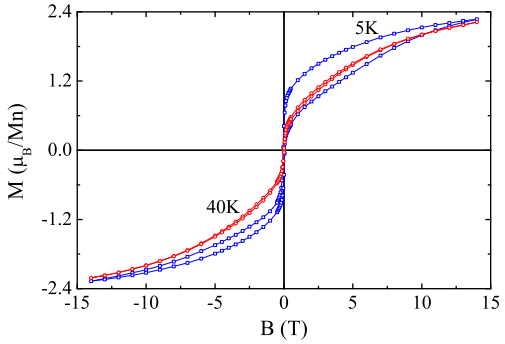

Fig. 2. Field dependencies of magnetization for $La_{0.7}Sr_{0.3}Mn_{0.85}Mg_{0.15}O_3$ samples measured at 5 K and 40 K.

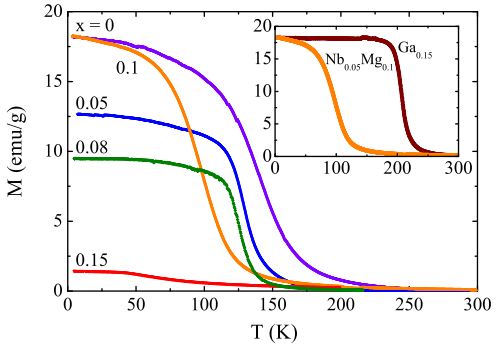

Fig. 3. Temperature dependencies of magnetizations for $La_{0.7}Sr_{0.3}Mn_{0.85}Nb_{0.15-x}Mg_xO_3$ and $La_{0.7}Sr_{0.3}Mn_{0.85}Ga_{0.15}O_3$ (inset) samples measured in a field of 0.02 T.

lower than the expected value for a pure ferromagnetic state. A rise in temperature suppresses the magnetic hysteresis. Note that a noticeable hysteresis in large magnetic fields has been detected as well for the $x = 0.1$ sample (Fig. 1).

The temperature dependencies of magnetization measured in a small magnetic field upon cooling are presented in Fig. 3. One can see that substitution of Nb ions by Mg ones results in a lowering of the Curie temperature which is maximal ($T_C = 150\ K$) for the formally Mn^{4+} free compound ($x = 0$). The $x = 0.15$ composition does not exhibit a pronounced anomaly on temperature dependence of magnetization thus indicating a possible magnetic inhomogeneity. Both $La_{0.7}Sr_{0.3}Mn_{0.85}Nb_{0.05}Mg_{0.1}O_3$ and $La_{0.7}Sr_{0.3}Mn_{0.85}Ga_{0.15}O_3$ contain formally an equal amount of Mn^{4+} ions (35%). However, the Curie point of the Ga-containing compound is significantly higher (inset in Fig. 3). These data show that the Mn^{4+} content is not the unique factor controlling ferromagnetism.

NPD measurements show that the crystal structure of all the samples at room temperature can be successfully described in the frame of the rhombohedral space group $R\bar{3}c$. However, the samples with Mg content in the range $0 \leqslant x \leq 0.08$ show a structural transition with decreasing temperature. This transition in the $x = 0$ and $x = 0.05$ compounds occurs above 200 K and 150 K respectively as evidenced by NPD. Rietveld refinement of the neutron diffraction patterns at low temperature has been performed for these compounds using the *Pnma* space group resulting in a good agreement between experimental data and calculated patterns (Fig. 4). The lattice parameters decrease smoothly with Mg doping (Table 1). As the ionic radius of Mg^{2+} is larger than that of Nb^{5+} the decrease of the unit cell volume is the result of the appearance of Mn^{4+} ions, which have a much smaller ionic radius than Mn^{3+} ones. The connection between the lattice and orbital degrees of freedom, as investigated in several orthorhombic manganites [16,19], suggests that the development of orbital ordering results in a contraction of the b parameter, and if $b/\sqrt{2} < c \leqslant a$ the occurrence of orbital ordering can be conjectured [16,19]. On the other hand, if $c > a \approx b/\sqrt{2}$, orbital disorder is expected. The observed relationship between the here determined structural parameters (Fig. 5) is in agreement with the absence of orbital order in the orthorhombic samples. The samples $x = 0.1$ and 0.15 have rhombohedral symmetry down to helium temperature. Rietveld refinement of the neutron diffraction patterns using high-resolution data indicates that the refined oxygen contents correspond to a stoichiometric composition (Table 1).

The additional intensity contribution to some structural peaks observed below 150 K for the $x = 0$ sample is associated with the ferromagnetic ordering (inset of Fig. 4a). The refined magnetic moment is 3.1 μ_B/Mn. Mg-doping leads then to a gradual decrease of the magnetic moment value (Table 1). The dependencies of the

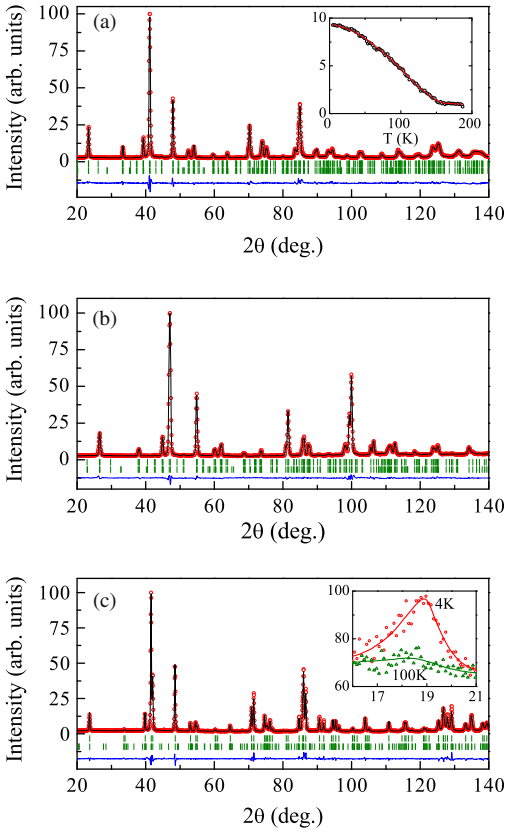

Fig. 4. Neutron powder diffraction patterns recorded at 2 K for $La_{0.7}Sr_{0.3}Mn_{0.85}Nb_{0.15}O_3$ (a), $La_{0.7}Sr_{0.3}Mn_{0.85}Mg_{0.08}Nb_{0.07}O_3$ (b), $La_{0.7}Sr_{0.3}Mn_{0.85}Mg_{0.15}O_3$ (c). The line and points refer to calculated and observed profiles, the bottom line represents their difference. The upper row of vertical ticks marks the Bragg reflections of the structural phase while the bottom row denotes ferromagnetic reflections. The inset of the top panel shows the temperature dependence of the triplet (002), (121) and (200). The inset of the bottom panel shows a magnified portion of the patterns at 4 K and 100 K of $La_{0.7}Sr_{0.3}Mn_{0.85}Mg_{0.15}O_3$ (D1B instruments).

Curie point and of the ferromagnetic moment value on the composition are shown in Fig. 5. For the $x = 0.15$ compound, one can notice that magnetic moment value determined from the ferromagnetic contribution to the Bragg peaks has decreased dramatically; indicating that only a very small fraction of the sample shows long-range ferromagnetic order. Moreover, at the position where A-type antiferromagnetic peaks normally appear, a broad hump can be noticed (Fig. 4c). This suggests the existence of short-range A-type antiferromagnetic regions in the sample. This

Table 1
The results of crystal and magnetic structures refinements of $La_{0.7}Sr_{0.3}Mn_{0.85}Nb_{0.15-x}Mg_xO_3$ samples.

T (K)	$x = 0$		$x = 0.08$		$x = 0.15$	
	10	300	2	300	10	300
Space group	*Pnma*	$R\bar{3}c$	*Pnma*	$R\bar{3}c$	$R\bar{3}c$	$R\bar{3}c$
a (Å)	5.521(1)	5.564(4)	5.495(7)	5.539(6)	5.493(5)	5.499(2)
b (Å)	7.810(2)	5.564(4)	7.774(2)	5.539(6)	5.493(5)	5.499(2)
c (Å)	5.557(7)	13.524(6)	5.541(1)	13.419(1)	13.297(1)	13.338(2)
V (Å^3)	239.63(1)	362.66(1)	236.73(7)	356.62(1)	347.52(1)	349.31(6)
V_p (Å^3)	59.9	60.44	59.18	59.44	57.92	58.22
La/Sr site	*4c*	*6a*	*4c*	*6a*	*6a*	*6a*
x	0.509(1)	0	0.507(7)	0	0	0
y	0.25	0	0.25	0	0	0
z	0.00001	0.25	0.003(1)	0.25	0.25	0.25
Biso (Å^2)	0.762(3)	1.066(3)	0.512(3)	0.624(4)	0.293(2)	0.458(2)
Mn/Mg/Nb (0,0,0) site	*4a*	*6b*	*4a*	*6b*	*6b*	*6b*
Biso (Å^2)	0.762(3)	1.066(3)	0.512(3)	0.624(4)	0.293(2)	0.458(2)
O1 site	*4c*	*18e*	*4c*	*18e*	*18e*	*18e*
x	−0.008(2)	0.548(1)	−0.006(3)	0.548(1)	0.544(2)	0.542(3)
y	0.25	0	0.25	0	0	0
z	−0.059(7)	0.25	−0.058(9)	0.25	0.25	0.25
Biso (Å^2)	0.838(6)	1.574(2)	0.627(4)	1.015(4)	0.673(2)	0.876(2)
Occupation	0.962(2)	1.004(4)	0.961(2)	1.007(2)	1.002(6)	0.992(4)
O2 site	*8d*		*8d*			
x	0.258(1)		0.259(7)			
y	0.031(2)		0.030(4)			
z	0.238(6)		0.238(9)			
Biso (Å^2)	1.273(4)		0.967(1)			
Occupation	1.016(1)		1.025(7)			
Some distances and angles						
Mn–O1 (Å)	1.981(1)	1.980(4)	1.971(1)	1.969(4)	1.949(8)	1.951(8)
Mn–O2 (Å)	1.961(7)/1.988(3)		1.960(8)/1.973(2)			
Mn–O1–Mn (deg.)	160.53(2)	164.48(2)	160.83(7)	164.46(1)	165.70(8)	166.31(1)
Mn–O2–Mn (deg.)	165.11(2)		165.40(3)			
Magnetic moment Mn ion						
μ_z (μ_B)	3.1		2.7		0.6	
R-factors						
R_p/R_{wp} (%)	5.08/6.58	4.56/5.95	3.74/4.95	3.01/3.95	5.23/6.85	4.96/6.26
R_{Bragg} (%)	6.07	3.54	4.44	3.03	4.45	3.88
Magnetic factor	11.5		9.89		9.21	

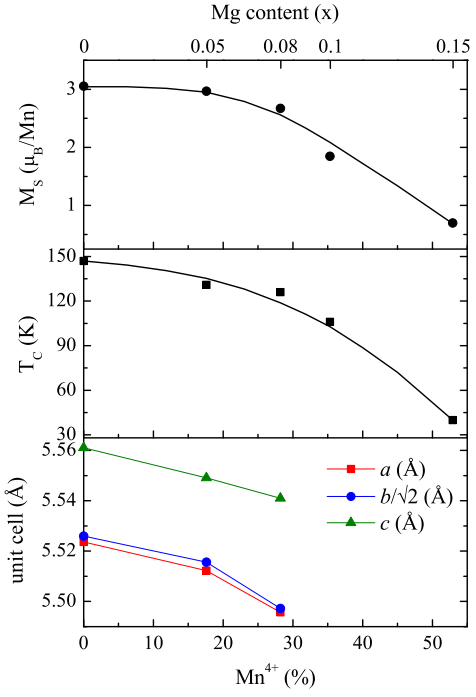

Fig. 5. Magnetic moment from NPD data (top panel), temperature Curie (middle panel) and unit cell parameters (bottom panel) vs. Mn^{4+} concentration for $La_{0.7}Sr_{0.3}Mn_{0.85}Nb_{0.15-x}Mg_xO_3$ samples.

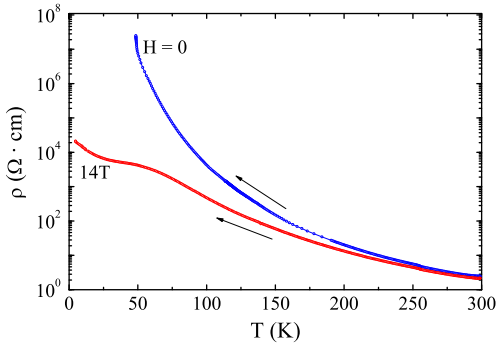

Fig. 6. Temperature dependence of resistivity for the $La_{0.7}Sr_{0.3}Mn_{0.85}Mg_{0.15}O_3$ sample.

antiferromagnetic short-range order disappears at around 100 K. Note that the antiferromagnetic ordering is not accompanied by significant changes in the crystal structure. Within experimental error the half width of the diffraction peak (024) is not dependent on temperature. This peak should split in orthorhombic or monoclinic symmetry.

All the samples show an insulating behavior of the resistivity. The $x = 0.15$ sample exhibits strong magnetoresistance (Fig. 6), however, its resistivity in a field of 14 T is still very large thus indicating the insulating character of the ferromagnetic phase.

4. Discussion

The determined structural parameters evidence that the orthorhombic distortion of the crystal lattice as found at low temperatures for the samples with 18% of Mn^{4+} ($x = 0.05$) and 27% of Mn^{4+} ions ($x = 0.08$) is not caused by a long-range orbital ordering. Unit cell parameters corresponds to *O*-type phase and smoothly decrease with Mg doping within the whole orthorhombic range $0 \leqslant x \leq 0.08$ (Fig. 5). Apparently the orthorhombic distortion is caused by steric effects similar to the case in optimally doped $La_{1-x}Ca_xMnO_3$ [30], where the *O*-type orthorhombic distortion points as well to an orbitally disordered state.

In contrast to the $La_{1-x}A_xMnO_3$ series (A = Ca, Sr, Ba) there is no enhancement of ferromagnetism under $Mg^{2+}(Mn^{4+})$ doping (Figs. 1, 3, 5). The conductivity is not strongly affected by the creation of Mn^{4+} through doping. Therefore, the ferromagnetism of the studied samples cannot be caused by orbital ordering or double exchange and is not associated with charge carriers. According to the Goodenough–Kanamori rules the sign of the 180-superexchange interaction between $Mn(e_g)$–O–$Mn(e_g)$ could not be determined for the Mn^{3+} ion if the orbital ordering is removed [18,20]. So, the antiferromagnetic and ferromagnetic components of the interactions can be equal. However, this statement is correct only in the case of a purely ionic bond. If, however, the chemical bond includes a covalent component hybridization occurs between the e_g orbitals of manganese and the *2p* orbitals of oxygen. This results in a decreasing formal population of filled e_g orbitals of Mn as e_g electrons are partially located at the oxygen site leading to an increase of the ferromagnetic component of the superexchange interactions. In the ionic model a similar effect results by partially replacing La^{3+} ions with two-valent alkaline earth ions, in this case Mn^{4+} ions appear. This substitution leads to the decrease of the antiferromagnetic contribution in the superexchange interactions as the e_g orbitals of Mn^{4+} are empty. Our assumption is in agreement with the structural and magnetic properties of the $La_{1-x}Tb_xMn_{0.5}Sc_{0.5}O_3$ series [31]. According neutron diffraction data $LaMn_{0.5}Sc_{0.5}O_3$ develops a true long range ferromagnetic ordering while $x = 0.5$ composition is spin glass [31]. The substitution of La with Tb causes a contraction in the unit cell volume that mainly reduces the M–O–M bond angle (M = Mn, Sc) while the M–O distance remains unchanged. The bending of this angle decreases the Mn–O–Mn ferromagnetic interaction and enhances the contribution from antiferromagnetic interactions. Accordingly, the magnetic ground state changes from ferromagnetic to a glassy magnetic state. The M–O–M angle controls *d*–*p* hybridization in perovskites [32].

On the other hand structural disorder can decrease the covalency due to local variations of the bond angle Mn–O–Mn. This angle controls the hybridization of *2p*(O) and it 3d(Mn) orbitals [20]. There is a critical value of the Mn–O–Mn angle associated with a change in sign of the superexchange interaction from positive to negative [20,33]. Mg^{2+} doping does not change the average angle Mn–O–Mn (Table 1), however, as the Mg^{2+} ion has an ionic radius much larger than Mn^{3+}, the doping with Mg^{2+} results apparently to some of the Mn–O–Mn angles being locally decreased below a critical value. As a consequence the optimal Mn^{4+} doping level in this system is formally close to zero. One can expect that Nb^{5+} doping leads as well to large structural disorder as Nb^{5+} has a relatively large ionic radius and a high oxidation state. In contrast to the Mg^{2+} and Nb^{5+} ions the Ga^{3+} ion has an ionic radius intermediate between Mn^{3+} and Mn^{4+}. The decrease of structural disorder in $La_{0.7}Sr_{0.3}Mn_{0.85}Ga_{0.15}O_3$ as well as the increase Mn–O–Mn angle enhance in this compound the Curie point in comparison to the $x = 0.1$ sample in spite of equal Mn^{4+} content (Fig. 3).

The $x = 0.15$ compound is in the half doped regime, containing about 50% Mn^{4+} ions. Hence one can expect that an antiferromagnetic component arising from t_{2g} electrons comparable with the ferromagnetic component should be present. However, there is no charge or orbital ordering because a large amount of Mg ions are randomly distributed over the lattice and the macroscopic symmetry remains rhombohedral down to 10 K. Remembering that rhombohedral symmetry does not allow any orbital ordering the A-type short-range antiferromagnetic order visible in this compound (inset of Fig. 4c) is likely caused by local distortions of the crystal structure. Assuming the antiferromagnetic clusters to have a small monoclinic distortion, this distortion would lead to a small anisotropy of the manganese electronic density associated with a compression of the MnO_6 octahedron which would probably be sufficient for the realization of A-type antiferromagnetic ordering. The magnetization data show (Fig. 2) that an applied field transforms the antiferromagnetic structure into a ferromagnetic one leading to a corresponding colossal magnetoresistance (Fig. 6). At the same time, however, the ferromagnetic phase remains in an insulating state due to the large amount of Mg^{2+} (Fig. 6).

Let us consider now in a more general way the possible role of superexchange in the establishment of ferromagnetism in metallic manganites. According to spectroscopic studies the electronic density of states near the Fermi surface is very small due to a pseudogap caused by strong correlation effects and disorder [34]. This is in agreement with theoretical considerations showing the majority of e_g electrons in manganites in the metallic state to be localized [35]. In this case the ferromagnetism can be strongly supported by positive exchange interactions associated with virtual excitations of e_g electrons in orbitals of nearest Mn^{3+} and Mn^{4+} ions. Such a hypothesis correlates well with the magnetic phase diagrams of half-doped manganites. In these manganites antiferromagnetic and ferromagnetic components of magnetic interactions are quite similar in size, so that insignificant changes of system parameters can lead to a transition from the antiferromagnetic into the ferromagnetic state and to the occurrence of a CMR effect [36]. The realization of a metallic antiferromagnetic state of A-type with a high Neel point [36] is in good agreement with a localized character of a majority e_g-electrons and an insignificant role of charge carriers in magnetic interactions. Indeed CE-type antiferromagnetic clusters have been found well above the Curie point of $La_{0.7}Ca_{0.3}MnO_3$ [37]. The competition between antiferromagnetic and ferromagnetic interactions in this compound can result in a first order paramagnet–ferromagnet transition and CMR effect.

The competition between antiferromagnetic and ferromagnetic interactions is a key factor for CMR in cobaltites, too [38,39]. The magnetic and transport properties of cobaltites can be understood assuming a localized character of the e_g electrons and a superexchange scenario for ferromagnetism [38,39]. It was suggested that metallicity in cobaltites arises from holes in the wide *2p* oxygen band because there is no evidence for an intergrain tunneling magnetoresistance [38]. In contrast to cobaltites the $CaCu3Mn_4O_{12}$-type perovskites exhibit a the large intergrain magnetoresistance [40]. This is in agreement with a large spin polarization of charge carriers. However, these compounds are ferromagnets due to the strong negative superexchange between copper and manganese ions [40]. So a large spin polarization of charge carriers is not a signature of double exchange.

We will now try to discuss the interplay between magnetism and orbital ordering. The orbital order–disorder transition in the parent compounds $LnMnO_3$ (Ln–lanthanide) has a martensitic character [18,41,42]. This means that there is a two phase regime under both doping and temperature variation. The orbitally ordered $LaMnO_3$ is A-type antiferromagnetic while the orbitally disordered $LaMnO_3$ has isotropic ferromagnetic interactions [18,43]. The experimental data for lightly doped $La_{1-x}A_xMnO_3$ (A = Ca, Sr; $x < 0.15$) provide no evidence for any homogeneous

ferromagnetic state within a formally d_{z^2}-orbital ordered phase [5–13,44]. Moreover the ferromagnetic ordering in the lightly doped manganites leads to a magnetostructural first-order transition into a less distorted low temperature phase and concomitant localization of the charge carriers [8,10,13]. The magnetostructural transition is accompanied by a significant increase of the spontaneous magnetic moment [8,10,13]. However, the low temperature phase is not homogeneous either. It contains inclusions of pure A-type antiferromagnetic phase as it was evidenced by NMR [7] and NPD [11] methods. Naturally one can suggest that these A-type antiferromagnetic inclusions arise from the local d_{z^2} orbital ordering inherent to parent $LaMnO_3$. So the static d_{z^2} orbital ordering seems to be incompatible with a pure ferromagnetic ordering in spite of mixing of d_{z^2} and $d_{x^2-y^2}$ orbitals.

The ferromagnetic state in single-valent manganites likely arises as well from the removal of the static Jahn–Teller distortion. It was suggested that a formally Jahn–Teller distorted $LaMn_{0.5}Ga_{0.5}O_3$ $\left(b/\sqrt{2} < c < a\right)$ is a homogeneous ferromagnet [12,15]. We suppose, however, that this compound is as well magnetically inhomogeneous. In fact the magnetic susceptibility of $LaMn_{0.5}Ga_{0.5}O_3$ strongly increases under pressure of 2.7 GPa [15] which could indicate that the compound contains antiferromagnetic clusters at ambient pressure [45]. External pressure transforms them into ferromagnetic ones thus leading to a decrease of the magnetic anisotropy. Indeed the structural study has shown that the increase in the magnetic susceptibility is accompanied by specific changes in the unit cell parameters as expected for an orbital order–disorder transition [15]. We suggest that the increase of the magnetic susceptibility is associated with the removal of the Jahn–Teller distortion. In comparison to $LaMn_{0.5}Ga_{0.5}O_3$ the completely orbitally disordered $LaMn_{0.4}Ga_{0.6}O_3$ is characterized by a larger Weiss constant thus indicating an enhancement of the ferromagnetic correlations [12]. In single-valent series $LaMn_{1-x}Cr_xO_3$ XAS data indicate for $LaMn_{0.9}Cr_{0.1}O_3$ the persistence of a strong static Jahn–Teller distortion around the Cr^{3+} ions [46]. The XAS data [46] were interpreted as reflecting the fact that the isolated Cr^{3+} ions at low doping values do not alter the local environment of Mn or the Mn–O–Mn superexchange interaction; neither the orbital order nor the magnetization are affected strongly. The breakdown of the orbital ordering should result at higher doping levels from a segregation of Cr ions into clusters. In fact the ferromagnetic component in the lightly doped $LaMn_{1-x}Cr_xO_3$ ($x < 0.15$) is much smaller in comparison with the orbitally disordered compositions $x = 0.4$ and $x = 0.5$ [19]. Note that the (Mn^{3+})–O–(Cr^{3+}) and (Cr^{3+})–O–(Cr^{3+}) magnetic interactions are antiferromagnetic [19,46]. This means that ferromagnetism is not stabilized by Cr^{3+}-related magnetic interactions [19]. It appears through the stabilization of the ferromagnetic (Mn^{3+})–O–(Mn^{3+}) interaction once the Jahn–Teller distortion has been removed due to a sufficient presence of Cr^{3+} ions. One can suggest that Ga^{3+} and Cr^{3+} doping leads to nanoscale structural separation into nanodomains with fast and low orbital dynamic. In the case of the temperature driven macroscopic structural phase separation in $LnMnO_3$ compounds the orbitally ordered and disordered domains have been detected by X-ray diffraction experiment in wide temperature range [42]. Our consideration indicates that the phase coexistence scenario corresponds to the published experimental data and ferromagnetism is stabilized by removal of the structural distortion associated with the d_{z^2} orbital ordering.

5. Conclusions

We have presented a detailed magnetic analysis of the doping effect of Mn^{4+} ions in the $La_{0.7}Sr_{0.3}Mn_{0.85}Nb_{0.15-x}Mg_xO_3$ system. The parent compound ($x = 0$) is basically ferromagnetic in spite of a formally single-valent Mn^{3+} state. The substitution of Nb^{5+} with Mg^{2+} is accompanied by an increase of the average manganese valence. The structural refinement shows that all the compositions are orbitally disordered. The increase of Mg^{2+} content leads to a weakening of the ferromagnetic interactions and stabilizes gradually the antiferromagnetic ones, in spite of the increase of Mn^{4+} content. The $x = 0.15$ (55% Mn^{4+}) compound exhibits a metamagnetic behavior associated with the transformation of A-type short-range order into ferromagnetic one. The ferromagnetism of manganese single-valent compounds can be understood in terms of the superexchange scenario and orbital disorder assuming a dominant role of covalency. It is suggested that a large local variation of the Mn–O–Mn bond angle due to Nb^{5+}/Mg^{2+} substitution destabilizes the ferromagnetic component. This angle is the key factor for p–d orbital hybridization and, hence, ferromagnetism. From our experimental data we do not see any need to invoke the strong double exchange interaction between Mn^{3+} and Mn^{4+} ions. Ferromagnetism in optimally doped mixed-valence manganites can be strongly supported by positive superexchange interactions between localized e_g electrons.

Acknowledgement

The authors would like to thank J.B. Goodenough for the fruitful discussion. This work has been supported by Belarusian Republican Foundation for Fundamental Research (Grant F14R-040).

References

[1] E. Dagotto, T. Hotta, A. Moreo, Colossal magnetoresistant materials: the key role of phase separation, Phys. Rep. 344 (2001) 1–153, http://dx.doi.org/10.1016/S0370-1573(00)00121-6.
[2] C. Zener, Interaction between the d-shells in the transition metals. II. Ferromagnetic compounds of manganese with perovskite structure, Phys. Rev. 82 (1951) 403–405, http://dx.doi.org/10.1103/PhysRev.82.403.
[3] C. Şen, G. Alvarez, E. Dagotto, Competing ferromagnetic and charge-ordered states in models for manganites: the origin of the colossal magnetoresistance effect, Phys. Rev. Lett. 98 (2007) 127202, http://dx.doi.org/10.1103/PhysRevLett.98.127202.
[4] P.G. de Gennes, Effects of double exchange in magnetic crystals, Phys. Rev. 118 (1960) 141–154, http://dx.doi.org/10.1103/PhysRev.118.141.
[5] G. Allodi, R. De Renzi, G. Guidi, F. Licci, M.W. Pieper, Electronic phase separation in lanthanum manganites: evidence from ^{55}Mn NMR, Phys. Rev. B 56 (1997) 6036–6046, http://dx.doi.org/10.1103/PhysRevB.56.6036.
[6] K. Kumagai, A. Iwai, Y. Tomioka, H. Kuwahara, Y. Tokura, A. Yakubovskii, Microscopically homogeneous magnetic structure of $La_{1-x}Sr_xMnO_3$ beyond the range of $0 < x < 0.1$ observed by La NMR, Phys. Rev. B 59 (1999) 97–99, http://dx.doi.org/10.1103/PhysRevB.59.97.
[7] K.-Y. Choi, H. Zhou, P. Kuhns, A. Reyes, N.S. Dalal, ^{55}Mn NMR study of $La_{1-x}Sr_xMnO_3$ ($x = 0.13$), Physica B 405 (2010) 390–393, http://dx.doi.org/10.1016/j.physb.2009.08.095.
[8] G. Biotteau, M. Hennion, F. Moussa, J. Rodríguez-Carvajal, L. Pinsard, A. Revcolevschi, Y.M. Mukovskii, D. Shulyatev, Approach to the metal–insulator transition in $La_{1-x}Ca_xMnO_3$ ($0 < x < 0.2$): Magnetic inhomogeneity and spin-wave anomaly, Phys. Rev. B 64 (2001) 104421, http://dx.doi.org/10.1103/PhysRevB.64.104421.
[9] U.H. Bents, Neutron diffraction study of the magnetic structures for the perovskite-type mixed oxides La (Mn, Cr)O_3, Phys. Rev. 106 (1957) 225–230, http://dx.doi.org/10.1103/PhysRev.106.225.
[10] M. Hennion, F. Moussa, The precursor phase of the CMR metallic state probed by spin and lattice dynamics, New J. Phys. 7 (2005) 84, http://dx.doi.org/10.1088/1367-2630/7/1/084.
[11] H.-F. Li, Y. Su, Y.G. Xiao, J. Persson, P. Meuffels, T. Brückel, Crystal and magnetic structure of single-crystal $La_{1-x}Sr_xMnO_3$ ($x \approx 1/8$), Eur. Phys. J. B 67 (2009) 149–157, http://dx.doi.org/10.1140/epjb/e2009-00019-5.
[12] J. Blasco, J. García, J. Campo, M.C. Sánchez, G. Subías, Neutron diffraction study and magnetic properties of $LaMn_{1-x}Ga_xO_3$, Phys. Rev. B 66 (2002) 174431, http://dx.doi.org/10.1103/PhysRevB.66.174431.
[13] A. Korolyov, V. Arkhipov, V. Gaviko, Y. Mukovskii, A. Arsenov, T. Lapina, S. Bader, J. Jiang, V. Nizhankovskii, Magnetic properties and magnetic states in $La_{0.9}Sr_{0.1}MnO_3$, J. Magn. Magn. Mater. 213 (2000) 63–74, http://dx.doi.org/10.1016/S0304-8853(99)00786-6.
[14] M.Y. Kagan, A.V. Klaptsov, I.V. Brodsky, K.I. Kugel, A.O. Sboychakov, A.L. Rakhmanov, Nanoscale phase separation in manganites, J. Phys. A: Math. Gen. 36 (2003) 9155, http://dx.doi.org/10.1088/0305-4470/36/35/304.
[15] J.-S. Zhou, Y. Uwatoko, K. Matsubayashi, J.B. Goodenough, Breakdown of magnetic order in mott insulators with frustrated superexchange interaction, Phys. Rev. B 78 (2008) 220402, http://dx.doi.org/10.1103/PhysRevB.78.220402.